Vision-Based Measurement of Two-Dimensional Positioning Errors of Machine Tools

AUTHOR(S):

IBARAKI, Soichi; TANIZAWA, Yusuke

CITATION:

IBARAKI, Soichi ...[et al]. Vision-Based Measurement of Two-Dimensional Positioning Errors of Machine Tools. Journal of Advanced Mechanical Design, Systems, and Manufacturing 2011, 5(4): 315-328

ISSUE DATE:

2011

URL:

http://hdl.handle.net/2433/152057

Vol.X, No.X, XXXX

Vision-based Measurement of Two-dimensional Positioning Errors of Machine Tools*

Soichi IBARAKI** and Yusuke TANIZAWA**
** Department of Micro Engineering, Kyoto University
Yoshida-honmachi, Sakyo-ku, Kyoto, 606-8501, Japan
E-mail: ibaraki@prec.kyoto-u.ac.jp

Abstract

This paper presents vision-based measurement of two-dimensional positioning errors of machine tools. A pre-calibrated grid plate is used as an artefact. The position of a grid point is measured in an image captured by a charge coupled device (CCD) camera attached to a spindle. Unlike conventional two-dimensional digital scales, the vision-based measurement can target the artefact in any orientation, and thus can be also applied to error calibration of a rotary axis. A longer working distance between the lens and the target is also its potential advantage for safer measurement. The paper demonstrates experimental applications of the vision-based measurement to the measurement of 1) static and 2) dynamic error motions of 1) a linear axis and 2) a rotary axis of a machine tool.

Key words : Vision-based measurement, volumetric accuracy, camera, grid, five-axis machining center.

1. Introduction

The technical sub-committee in ISO (International Organization of Standardization), ISO TC39/SC2, has been lately discussing on the publication of a Technical Report (TR) on the numerical compensation of volumetric errors of machine tools[(1)]. Such an effort clearly indicates recent recognition of the importance of volumetric accuracy by machine tool manufacturers and users. In ISO/FDIS 230-1:2011[(4)], under a revision process at ISO TC39/SC2, the definition of the term "volumetric accuracy" is newly added as "maximum range of relative deviations between actual and ideal position in X-, Y- and Z-axis directions and maximum range of orientation deviations for A-, B- and C-axis directions for X-, Y- and Z-axis motions in the volume concerned." The objective of the volumetric error compensation is to cancel an error in the tool center position (TCP) at an arbitrary point in the entire workspace by adjusting the command position. Its application to machine tools has been long studied[(2), (3)], and many of major CNC makers recently commercialized such a functionality. They typically adopt some form of the model-based compensation, where the machine's kinematic model is assumed to predict the positioning error at an arbitrary point.

For volumetric error compensation, the construction of the machine's kinematic model is thus crucial. According to Schwenke et al.[(2)], the "direct" measurement of geometric errors represents the analysis of single errors. Many machine tool calibration tests widely done in the industry, e.g. the measurement of linear positioning errors by using a laser interferometer, are direct measurements. For the kinematic model construction, the inefficiency of the direct measurement can be a critical issue. For orthogonal three-axis machines, 3 linear positioning errors, 6 straightness errors, 3 squareness errors, 6 angular errors must be measured by different setups to construct the machine's kinematic model.

The "indirect" measurement focuses on the tool tip location as the superposition of these single errors. In early attempts, indirect methods have been developed as a a quick check of the machine's motion accuracy. More researchers recently reported the application of indirect

* Received DD MM, YYYY (No. XX-XXXX)

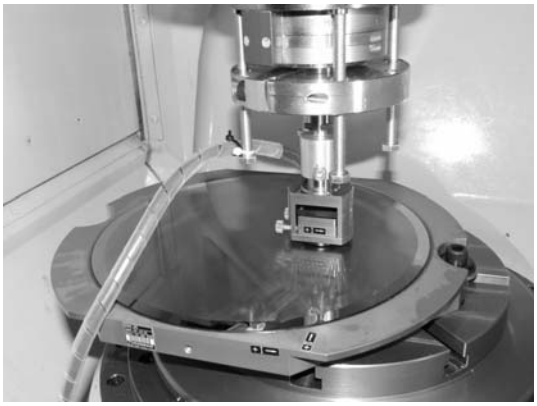

Fig. 1 A two-dimensional digital scale, KGM 182 by Dr. Johannes Heidenhain GmbH.

measurements to the construction of the kinematic model. For its efficient construction, it is important to measure the TCP *at arbitrary locations* within the work volume. Many typical indirect measurements, e.g. circular tests by the ball bar[5), 6)], do not allow the measurement at an arbitrary position (for example, only a circular trajectory can be tested by the ball bar). Only measuring instrument commercially available with the capability to measure arbitrary trajectories in three-dimensional space is, to the authors' knowledge, a tracking interferometer (laser tracker)[7)–9)]. Its acceptance by machine tool builders is, however, still very limited due to its higher cost and the difficulty to ensure its accuracy.

For *two-dimensional* TCP measurement on arbitrary trajectories, a two-dimensional digital scale[4)], or a cross grid encoder (KGM), is commercially available from a couple of companies including Dr. Johannes Heidenhain GmbH[10)] (see Fig. 1). It measures the position in two-dimensional orthogonal coordinate system by photoelectric scanning of a grid as the measurement reference[11)]. Although its acceptance by machine tool builders is still not as wide as ball bars, its application to the kinematic model construction, making use of its capability to measure arbitrary trajectories, has been studied in many papers[12)–14)].

Conventional two-dimensional digital scales have following inherent issues:

(1) The gap between the grid plate and the measuring head must be sufficiently small for photoelectric scanning. For example, Heidenhain recommends to set the gap about 0.5 mm[10)]. The setup must be, therefore, done carefully by an experienced operator. The misoperation may easily crash the grid plate.

(2) The orientation of the grid plate must be precisely aligned to the measuring head in order to obtain valid signal. Its setup may require significant time. More importantly, it cannot be used to measure error motions of a rotary axis.

(3) The calibration of a reference grid is very difficult in practice.

(4) It is difficult to manufacture a larger grid plate with required geometric accuracy. For example, the largest grid plate by Heidenhain is ϕ230 mm.

With technological advances in cameras and machine vision algorithms, many vision-based measurement systems are now available in a variety of industrial applications[15)]. The objective of this paper is to present the application of vision-based measurement to two-dimensional multi-axis (kinematic) tests for numerically controlled machine tools. The position of a spindle in relative to work table is measured by using a charge coupled device (CCD) camera attached to the spindle, viewing a pre-calibrated artifact fixed on the work table. Compared to conventional two-dimensional digital scales, vision-based measurement has following potential advantages:

(1) The distance between camera and object can be, depending on the working distance of lens, several tens of millimeters, which significantly facilitates the setup procedure and improves the safety.

(2) The measurement is possible even when the camera rotates to the object.

(3) It is easier to calibrate the artefact, and to make larger artefact with lower cost.

To the authors' knowledge, no research effort has been reported in the literature on the application of vision-based measurement to the calibration of machine tool volumetric accuracies. Experimental studies will be presented to demonstrate potential capabilities of vision-based measurement to the calibration of 1) static and 2) dynamic error motions of 1) a linear axis and 2) a rotary axis of a machine tool.

2. Vision-based two-dimensional position measurement

2.1. Measurement principle and artefact

The objective is to measure the displacement of the TCP relative to the work table. A glass plate, on which horizontal and vertical lines of metal are vacuum-deposited, is fixed on the work table as an reference artefact. A CCD camera is attached to the spindle.

In all tests presented in this paper, for the simplicity of the algorithm, the image size is set such that a single set of intersecting lines is captured in each image. The objective of the algorithm is to calculate the position of the intersection of images of vertical and horizontal reference lines (referred to as the grid point hereafter) in an image.

The contour (edge) detection is one of fundamental operations required in many image processing applications. Numerous efforts have been devoted to develop its reliable algorithms[(15)–(17)], many of which are now available in commercial image processing software. Since the object in our study is restricted to a simple grid, we employ a simple algorithm to calculate the position of the grid point in the captured image. The following subsection only briefly reviews the algorithm.

2.2. Measurement of grid point position

(1) Edge recognition in pixel-size resolution

The edge of a line is defined in the pixel-size resolution as a set of pixels where the first-order gradient of the pixel brightness is locally maximized. Figure 2 shows an illustrative example of the edge recognition in the pixel-size resolution. Figure 2(a) shows a captured image of the boundary of a line on the reference grid plate. The left side corresponds to the line reflecting the light. In each scanning line (a X-direction line in this example), the brightness profile is obtained as in Fig. 2(b). By using the Sobel operator[(17)], the gradient of pixel brightness is calculated as shown in Fig. 2(c). On each scanning line, the pixel maximizing its 2-norm is searched.

(2) Edge recognition in sub-pixel-size resolution

To identify the edge point in a resolution smaller than the pixel size, the norm of the gradient of pixel brightness is computed at all the points adjoining to the point found in (1). Then, as illustrated in Fig. 3, a polynomial surface to interpolate them is calculated. Its local maximum is calculated at the scanning line in a resolution of one tenth of the pixel size.

(3) Calculation of grid point

The grid point is defined as illustrated in Fig. 4. Straight lines representing both edges of the image of a reference line, represented by l_{A1} and l_{A2} (or l_{B1} and l_{B2}) in Fig. 4, are calculated by least-square fitting a set of edge points calculated in (2). The mean line of l_{A1} and l_{A2} (l_{B1} and l_{B2}) is given by the line l_{A3} (l_{B3}). The grid point is defined as the intersection of l_{A3} and l_{B3}. The position of the grid point is calculated in the coordinate system attached to the captured image with the origin at the center of the image.

3. Experimental setup and target measurement performance

Tables 1, 2, and 3 respectively show major specifications of the camera, the lens, and the light, used in our experiment. Table 4 shows specifications of the grid plate. The grid plate is pre-calibrated (see Section 6). A commercial vertical five-axis machining center,

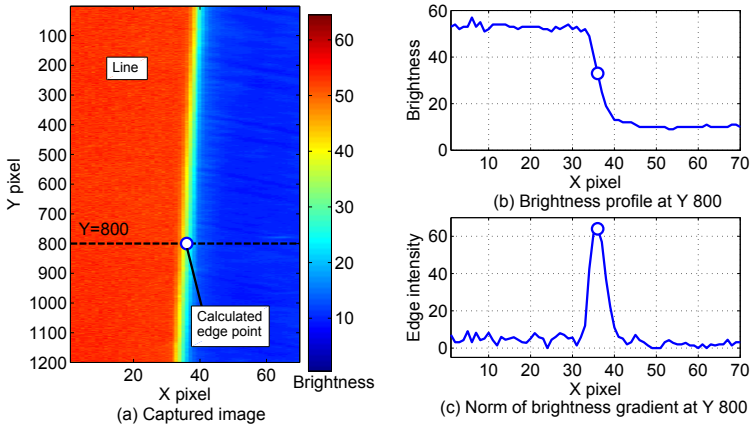

Fig. 2 An illustrative example of edge recognition in the pixel-size resolution.

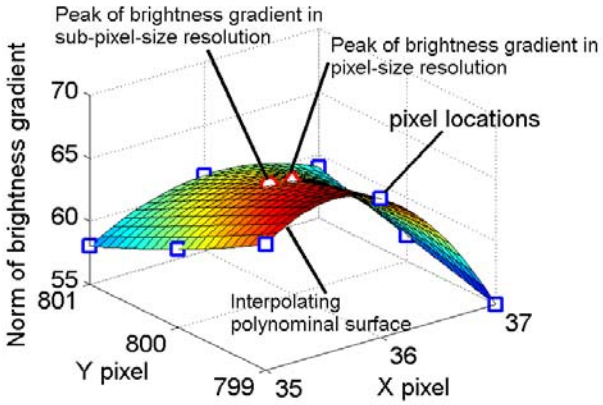

Fig. 3 An illustrative example of edge recognition in sub-pixel-size resolution.

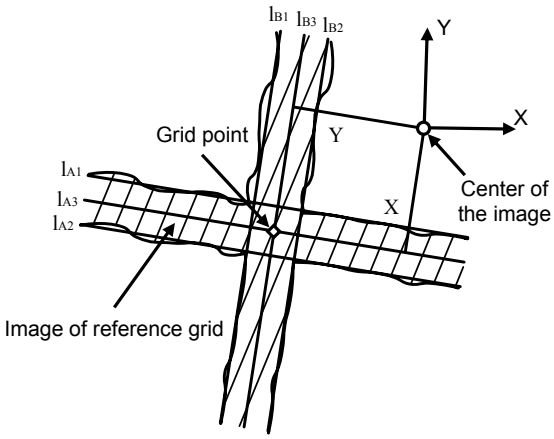

Fig. 4 Definition of grid point.

NMV1500DCG by Mori Seiki Co., Ltd., of the configuration shown in Fig. 5 is measured. Table 5 shows its major specifications.

Figures 6 and 7 show the experimental setup. The camera with the lens and the ring light guide is attached to the machine's spindle. A TTL signal is generated by a PC-based real-time controller (used just as a signal generator) and sent to the image capture board to trigger the image capture by the given period.

Major measurement performance targeted in this study is as follows:

(1) Measurement resolution:

The position measurement with the resolution 1 μm is targeted. From the pixel size of

Table 1 Specifications of camera

Name	Sensor Technology Co., Ltd. STC-CL500A
Image sensor	CCD (black-and-white)
Number of valid pixels	2456(H)× 2058(V) (About five million pixels)
Area of valid pixels	8.47 mm(H)× 7.10 mm(V)
Pixel size	3.45 μm(H) × 3.45 μm(V)
Shutter speed	1/8 to 1/209,000 sec
Data resolution	8/10/12 bits (12 bits in experiments)
Output interface	Cameralink
Image capture board	Grablink 1621 Express (by Euresys)

Table 2 Specifications of lens

Name	Seiwa Optical Co., Ltd. Zoom tube lens MS-501
Magnification	0.75× ~ 4.5×
Working distance	90 mm
Focal depth	1.8 mm ~ 0.129 mm
Distortion	0.5 %~0.1 %
Resolution	11.6 μm~ 4.9 μm
Numerical aperture (NA)	0.029~ 0.069
Camera mount	C-mount

Table 3 Specifications of light

Name	Seiwa Optical Co., Ltd. Fiber illuminator FA100-EN Ring light guide HL-28-2000
Light source	Halogen light source
Power consumption	130 W
Light guide	Ring-shaped
Light spot diameter and angle	32 mm, 10°

Table 4 Specifications of grid plate

Name	Pyser-SGI Ltd. PGR-200
Grid substrate	Vacuum-deposited chrome on glass
Plate size	160 mm×240 mm
Grid size	140 mm×220 mm
Grid pitch	10 mm
Line width	0.008 mm
Lines' orientation accuracy	≤ 5 arcsec

Table 5 Specifications of machining center

Name	Mori Seiki Co., Ltd., vertical-type 5-axis machining center, NMV1500DCG				
Axis	X	Y	Z	B	C
Stroke	420 mm	210 mm	400 mm	−180° ~ 160°	360°
Drive	Servo motor and ball screw			direct drive (DD)	
Positioning resolution	1 μm			1 mdeg	
Table size	ϕ 250 mm				

the camera in Table 1 and the lens magnification (fixed at 0.75× in all the tests), one pixel approximately corresponds to the area 6.6 μm×6.6μm (the view area is about 11.3 mm (H)×9.50 mm(V)). This means that 1 μm measurement resolution requires the edge recognition in the resolution of about 1/6.6 of the pixel size.

Considering that the positioning resolution of typical machining centers in today's market is 1 μm or even smaller, the measurement resolution of 1 μm may not be sufficient for practical applications. Due to the difficulty to investigate its measurement uncertainty in the sub-micrometer level by our experimental facilities (the machine tool's positioning resolution is 1 μm), this study limits the target measurement performance to this level. To obtain higher resolution, higher lens magnification should be used. In such a case, the lens distortion may impose larger influence on the measurement uncertainty. See Section 6 for further discussion.

(2) Measurable velocity in dynamic measurement:

Due to the limitation in sampling capabilities of the camera and the image capture board, the machine's feedrate is limited to 100 mm/min in dynamic measurement. When the shutter speed of the camera is set at 1/2,000 sec, the table moves by about 0.8 μm in 1/2,000 sec, smaller than the target measurement resolution. Although this maximum velocity is clearly insufficient for practical applications, this paper only presents preliminary tests to validate the feasibility of dynamic vision-based measurement. To perform the vision-based measurement for higher feedrate, a high-speed camera allowing higher shutter speed and faster image processing capability are needed.

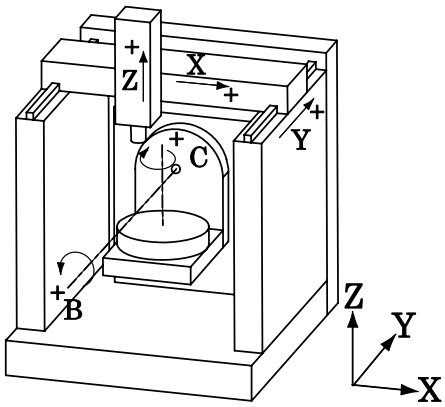

Fig. 5 Configuration of the machining center.

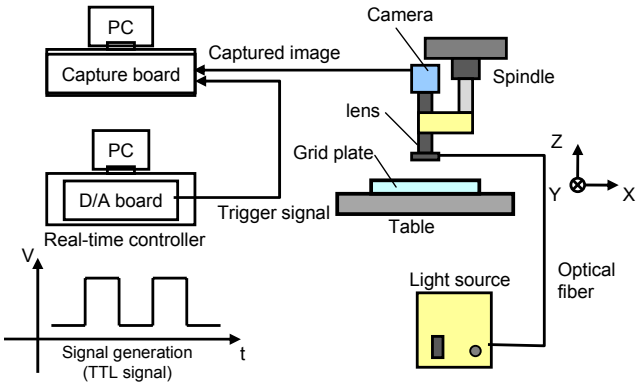

Fig. 6 Schematics of experimental setup.

Fig. 7 Experimental setup.

4. Case study I: Static tests

4.1. Case study I-1: Static positioning error measurement for linear axes

(1) Test procedure

Figure 8 illustrates the test setup. The origin of the coordinate system is set at the upper-left corner of the grid. Horizontal and vertical lines of the grid are aligned at every 10 mm. The machine is operated such that the camera is positioned along the horizontal line $Y = -20$ mm at $X = 0, 20, \cdots, 220$ mm (total 12 points). An image is captured at each stop position. This operation is repeated in both directions (i.e. $X = 0 \rightarrow 220$ and $X = 220 \rightarrow 0$) at three different Y locations, $Y = -20, -100, -120$ mm. Similarly, this set of measurement is done to the Y-direction ($Y = -140, -120, \cdots, 0$ mm, total 8 points) at three different X locations, $X = 10, 90, 180$ mm.

The image size is set such that only one intersection of horizontal and vertical lines is contained in captured images. Command positions are given such that the intersection is approximately at the center of the image at each stop position. The orientation of the camera to the grid plate is aligned only roughly. The positioning error in X- and Y-directions is measured by the position of the grid point in the image. Suppose that the pre-calibrated position of (i, j)-th grid point is given by $q^*_{ij} \in \mathbb{R}^2$ in the coordinate system shown in Fig. 8, and that the position of the grid point measured in the coordinate system attached to a capture image (see Fig. 4) is given by $\Delta p_{ij} \in \mathbb{R}^2$. Then, the measured TCP (camera) position in the coordinate system shown in Fig. 8, $p_{ij} \in \mathbb{R}^2$, is calculated by:

$$p_{ij} = q^*_{ij} - \Delta p_{ij} \tag{1}$$

The positioning error is set zero at $(X, Y) = (0. - 20)$ mm. Only the relative displacement from this position is evaluated.

(2) Measurement result

Figure 9 shows the measured "error map" of the two-dimensional static positioning error. The symbols • indicate command positions. The symbols ◯ and □ show measured positions, where an error from the command position is magnified 10,000 times in both X and Y directions. Each test is repeated three times, and mean positions are shown in Fig. 9. The coordinate system is re-defined such that the average line of measured positions at $Y = -100$ mm ($X = 0, \cdots, 220$) is aligned to its X-direction.

4.2. Case study I-2: Static measurement of radial error motions of a rotary axis

(1) Test procedure

Unlike conventional KGMs, the vision-based measurement can perform the measurement even when the target is rotated; this is its strong potential advantage. To demonstrate it, the vision-based static measurement of radial error motions of a rotary table (C-axis) is tested. Figure 10 illustrates its setup. The grid plate is fixed on the rotary table such that one of grid points is located approximately on the C-axis average line. The B-axis is clamped horizontally (at $B = 0°$). The grid position is manually adjusted such that the movement of the grid point concerned is minimized in captured images with the C-axis rotation. Since an offset of the camera to the spindle axis average line is unknown, the camera position is searched also from captured images such that this grid point is viewed approximately at the center of the image. Only one intersection of two lines is captured in the image.

The rotary table is indexed at total 21 angular positions, C_i ($i = 1 \sim 21$), in 360° rotation. The camera position is fixed throughout the test. The two-dimensional displacement of the grid point, $\Delta p_i \in \mathbb{R}^2$, is measured in each statically captured image at C_i. The relative displacement from the position measured at the the beginning of the test ($C_i = 0°$) is evaluated. Due to an alignment error of the grid plate to the C-axis average line, the observed grid point moves along a circular trajectory of small radius in captured images. This influence is removed by using the least square fit.

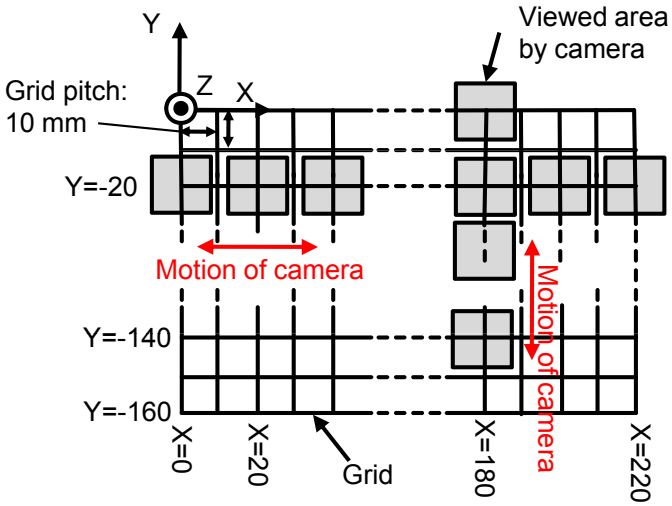

Fig. 8 Setup of static positioning error measurement for linear axes. Similar tests are done for horizontal lines, $Y = -20, -100, -120$ mm, and vertical lines, $X = 10, 90, 180$ mm.

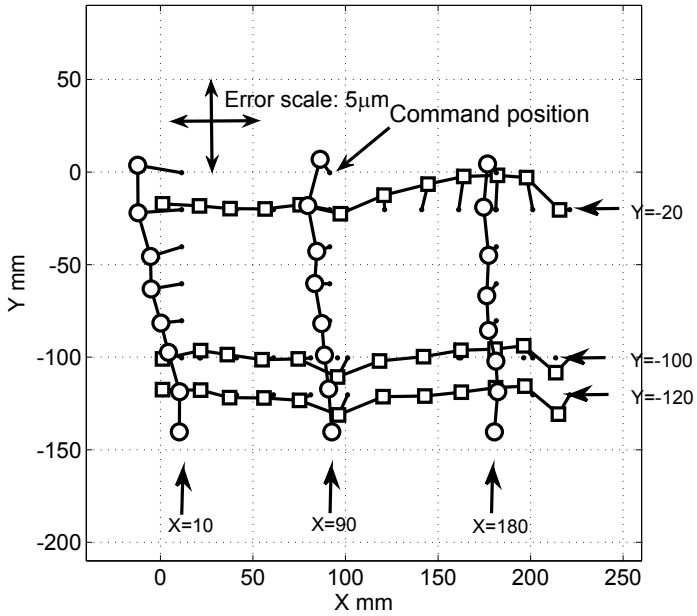

Fig. 9 Two-dimensional error map by vision-based measurement (error is magnified 10,000 times).

(2) Measurement result

This test only measures the static radial error motion of the rotary axis. The angular positioning error cannot be observed since the grid point is approximately on the axis of rotation. As is schematically illustrated in Fig. 11, the measured radial error motion of C-axis, i.e. the projection of the measured displacement in the radial direction to the C-rotation, is polar-plotted with respect to C_i. Figure 12 shows the measured radial error profile. Three repeated measurements are all shown. It can be observed that the static radial error motion of C-axis is within $\pm 1.2\mu$m.

5. Case study II: Dynamic tests

5.1. Case study II-1: Dynamic measurement for linear interpolations

(1) Test procedure

The test setup is analogous to that in Fig. 8 except for that the measurement is dynamic.

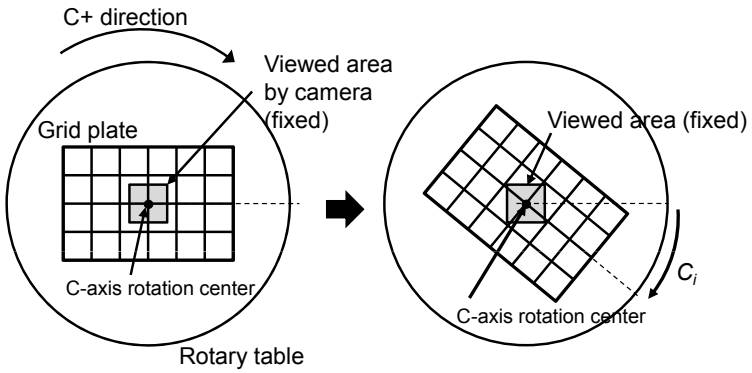

Fig. 10 Setup of vision-based measurement of radial error motion of a rotary table.

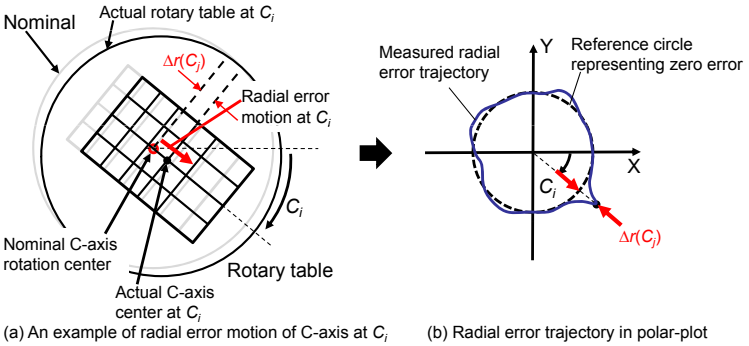

Fig. 11 Schematic of a polar plot of radial error motions (for easier understanding of Fig. 12)

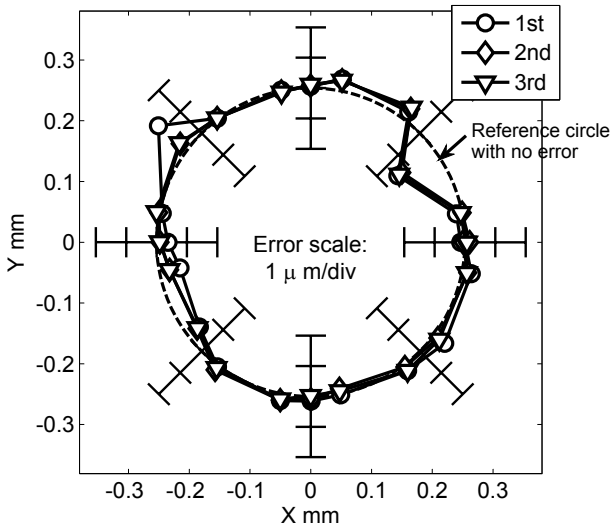

Fig. 12 Radial error motions of C-axis by the vision-based measurement.

The machine is operated such that the camera moves toward the X-direction with a constant feedrate 100 mm/min from $X = 0$ to 220 mm along a horizontal line, $Y = -100$ mm. At every 20 mm, an image of the grid point is captured as the camera keeps moving. The same operation is conducted as the machine moves to the Y-direction from $Y = -140$ to 0 mm along a vertical line $X = 180$ mm.

(2) Measurement result

Figure 13 shows position errors in the direction normal to the feed direction (i.e. contouring error) by the vision-based system. Although the measurement is dynamic, an image

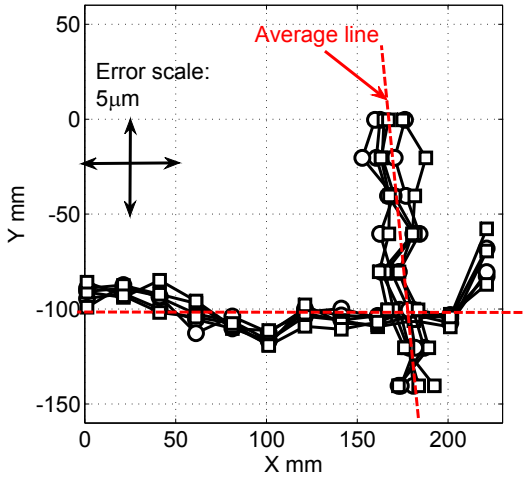

Fig. 13 Dynamic contour errors measured by the vision-based measurement system for straight paths at (i) $Y = -100$ mm and (ii) $X = 180$ mm. The error is magnified 10,000 times. ○ and □: measured camera positions at each grid point (for positive and negative feed directions).

is captured only by the interval 20 mm as described above. An error from the reference line is magnified 10,000 times. Three repeated measurements in both positive and negative feed directions are all shown.

5.2. Case study II-2: Dynamic measurement for circular interpolations

(1) Test procedure

A circular test, described in ISO 230-4:2005[5], is widely accepted by machine tool builders[6]. For latest small-sized, high-accuracy machine tools, a small-radius circular test is often of a practical interest since it clarifies the influence of the machine's dynamics[20]. A KGM is often used for such a small-radius circular test. This subsection presents the application of the vision-based measurement to a circular test.

Figure 14(a) illustrates the test setup. The grid plate is fixed on the machine table. The machine commands a circular interpolation of the radius 2.5 mm in the XY plane with the feedrate 100 mm/min. One grid point of the grid plate is located approximately at the center of the circular trajectory. Figure 14(b) illustrates its position in captured images. Since the trajectory's radius is smaller than the size of the captured image, the same grid point can be always observed in captured images as the camera goes along the entire circular trajectory. An image is captured with the sampling time 4 frame/sec as the camera keeps moving. By measuring the position of this grid point in each captured image, the camera's displacement to the reference circular trajectory can be calculated.

(2) Measurement result

Figure 15(a) shows the measured contour error profile by the vision-based system. For the comparison, Fig. 15(b) shows the error profile for the same circular path measured by using a commercial two-dimensional digital scale, KGM 182 by Dr. Johannes Heidenhain GmbH (Fig. 1). Figure 15(a) shows constant radial error of about 7 μm over the entire circular path, which is not in Figure 15(b). Its major contributor is the distortion of the camera lens. In this test, as seen in Fig. 14(b), the grid point concerned moves along a approximately circular path in captured images as the machine goes along the circular path. In all other tests (Case studies I-1, I-2, and II-1), the grid point concerned is always approximately at the center of captured images. Therefore, this is the only test presented in this paper where the lens distortion imposes significant influence on the test result. To clarify this issue, the lens distortion was not calibrated and compensated in this test. Further discussion will be presented in the following section.

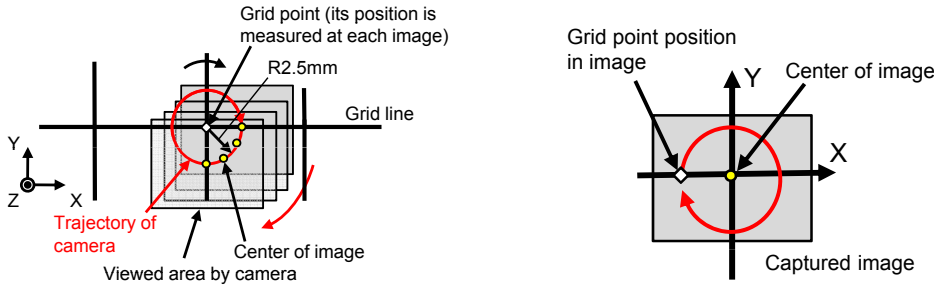

(a) Measurement setup on the machine. (b) Position of grid point in captured images.

Fig. 14 Setup of vision-based measurement of contour error for circular interpolation of small radius.

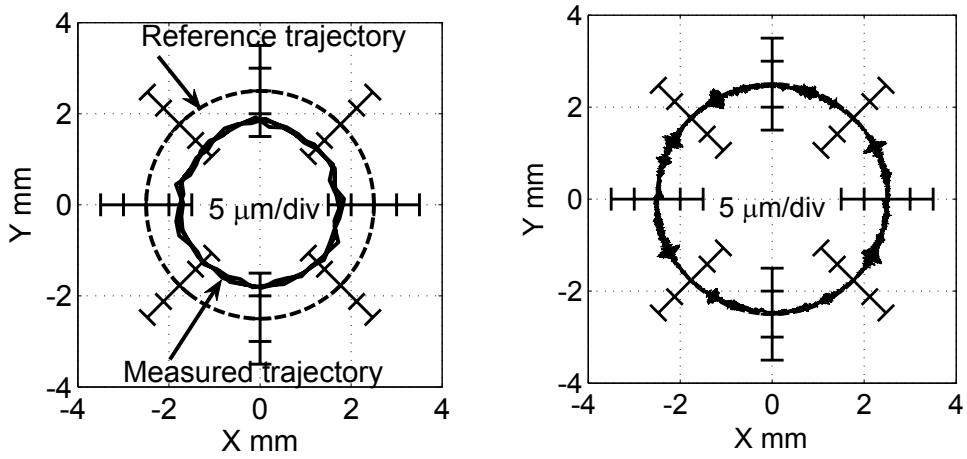

(a) Measured by using a vision-based system. (b) Measured by using a cross grid encoder.

Fig. 15 Measured dynamic contour errors for a circular path of the radius 2.5 mm under the feedrate 100 mm/min. The contour error is magnified 100 times.

6. Remarks on major contributors for measurement uncertainties

The measurement uncertainty in the vision-based measurement has been discussed in the literature[21)–23)]. Major contributors to the vision-based position measurement presented in this paper are the following factors. This section gives brief remarks on how these major contributors are dealt with in the present experimentation and issues to further extend the application of the vision-based measurement.

(1) Calibration error of the artefact

The position of each grid point of the grid plate must be pre-calibrated. In this paper, we calibrated the grid plate by using a commercial vision-based coordinate measuring machine, SmartScope VANTAGE 600 by Optical Gaging Products, Inc. Its volumetric uncertainty is calibrated by the manufacturer to be $1.5 + 4L/1000$ μm where L is the measurement length. The self-calibration of the grid is also possible[19), 24)].

In Case studies I-1 and II-1, an image is captured at multiple grid points. The grid calibration error is, therefore, directly copied as its measurement uuncertaintyOn the other hand, Case studies I-2 and II-2 keep watching the single grid point, and thus the grid calibration error does not contribute at all on the measurement uncertainty.

(2) Lens distortion of camera

In Case studies I-1, I-2, and II-1, the grid point is nominally at the center of each image. Therefore, the influence of the lens distortion on these tests is negligibly small. Only in Case study II-2, the grid point is off the center of each image, and thus the lens distortion potentially imposes significant contribution on the measurement uncertainty. Note that the geometric inaccuracy of CCD pixel arrays in the camera also imposes analogous influence on

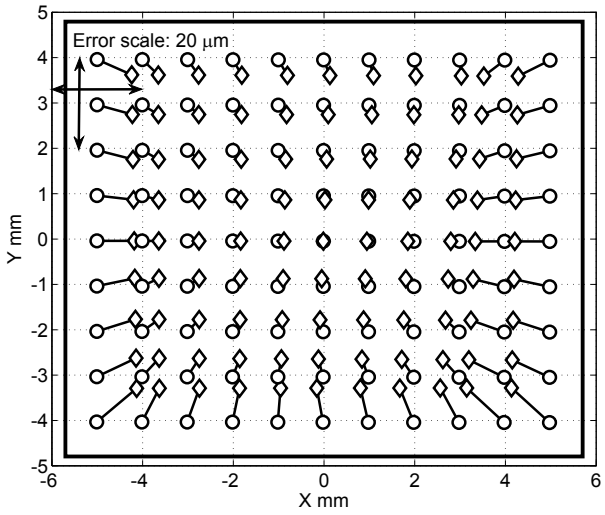

Fig. 16 Lens distortion observed by capturing an image of a pre-calibrated grid. ⋄: the measured position of each grid point in the captured image, ○: its pre-calibrated position. The error is magnified 100 times.

the measurement uncertainty.

To investigate the distortion of the lens used in present experiments, the following calibration was conducted: a glass grid plate of the pitch 1 mm (size: 10 mm×8 mm) was calibrated as described above. The camera was fixed approximately above the center of the grid plate. A single image was captured, and the position of each grid point was measured from the captured image. Figure 16 shows an error of the measured position of each grid point from its pre-calibrated position. Errors observed are mostly attributable to the lens distortion.

The conventional two-dimensional scale (KGM) measures the position of a single point in reference to the grid plate. Similarly, when the grid pitch is sufficiently small and an image was captured only on each grid point, the calibration of the lens distortion is not needed. In other words, when the lens distortion was properly calibrated and compensated, the grid pitch can be larger than conventional two-dimensional scales to obtain the same measurement resolution.

(3) Dynamics of measurement system

The present measuring system has much longer working distance (90 mm) than conventional two-dimensional digital scale. Therefore, the tilt error of the camera (lens) may potentially impose larger influence on the measurement uncertainty particularly in dynamic measurement. Dynamic displacement and tilting of the camera (lens tube) was not investigated in present experimentations (Case studies II-1 and II-2).

7. Conclusion

Unlike conventional two-dimensional digital scales, the vision-based measurement can target the artefact in any orientation. It can be therefore applied to the error calibration of a rotary axis in five-axis machine tools. A longer working distance between a lens to the target, and easier calibration of the artefact accuracy, as well as its lower cost, are also its potential advantages.

To demonstrate potential capabilities of vision-based measurement to machine tool calibration, this paper presented experimental studies on the measurement of 1) static and 2) dynamic error motions of 1) a linear axis and 2) a rotary axis of a machine tool.

Acknowledgement

The machining center used in present experiments is loaned by the Machine Tool Tech-

nologies Research Foundation (MTTRF) via Equipment on Loan Award Program. It is also in part supported by the JSPS Grants-in-Aid for Scientific Research (#23560122).

References

(1) ISO/PDTR 16907:2011, *Numerical compensation of geometric errors of machine tools*.
(2) H. Schwenke, W. Knapp, H. Haitjema, A. Weckenmann, R. Schmitt, and F. Delbressine, Geometric error measurement and compensation of machines –An update, *CIRP Annals – Manufacturing Technology*, Vol.57, No.2, (2008), pp.560-575.
(3) R. Ramesh, M. A. Mannan, and A. N. Poo, Error compensation in machine tools – a review: Part I: geometric, cutting-force induced and fixture-dependent errors, *International Journal of Machine Tools and Manufacture*, Vol.40, No.9, (2000), pp.1235-1256.
(4) ISO/FDIS 230-1:2011, *Test code for machine tools – Part 1: Geometric accuracy of machines operating under no-load or quasi-static conditions*.
(5) ISO 230-4:2005, *Test code for machine tools – Part 4: Circular tests for numerically controlled machine tools*.
(6) Y. Kakino, Y. Ihara, and A. Shinohara, *Accuracy Inspection of NC Machine Tools by Double Ball Bar Method*, (1993), Hanser Publishers.
(7) G. N. Peggs, Virtual technologies for advanced manufacturing and metrology, *International Journal of Computer Integrated Manufacturing*, Vol.16, No.7-8, (2003), pp. 485-490.
(8) H. Schwenke, M. Franke, J. Hannaford, and H. Kunzmann, Error mapping of CMMs and machine tools by a single tracking interferometer, *CIRP Annals - Manufacturing Technology*, Vol.54, No.1, (2005), pp. 475-478.
(9) T. Yano, T. Takatsuji, S. Osawa, T. Suzuki, Y. Motomura, and T. Itabe, Development of a Small Two Axis Spherical Motor Type Laser Tracker with Submicron Measurement Accuracy, *IEEJ Trans. on Sensors and Micromachines*, Vol.126, No.4, (2006), pp.144-149. (in Japanese)
(10) Dr. Johannes Heidenhain GmbH, *Measuring systems for machine tool inspection and acceptance testing (catalog)*, (2007).
(11) A. Teimel, Technology and Application of Grating Interferometers in High Precision Measurement, *Precision Engineering*, Vol.4, (1992), pp.147-154.
(12) W. Knapp and S. Weikert, Testing the contouring performance in 6 degrees of freedom, *Annals of the CIRP - Manufacturing Technology*, Vol.48, No.1, (1999), pp. 433-436.
(13) K. Lee, S. Ibaraki, A. Matsubara, Y. Kakino, Y. Suzuki, S. Arai, and J. Braasch, A Servo Parameter Tuning Method for High-speed NC Machine Tools based on Contouring Error Measurement, *Laser Metrology and Machine Performance VI*, WIT Press, (2002).
(14) Z. Du, S. Zhang, and M. Hong, Development of a multi-step measuring method for motion accuracy of NC machine tools based on cross grid encoder, *International Journal of Machine Tools and Manufacture*, Vol.50, No.3, (2010), pp. 270-280.
(15) A. Hornberg (editor), *Handbook of Machine Vision*, Wiley-VCH, (2006).
(16) G. Papari, N. Petkov, Edge and line oriented contour detection: State of the art, *Image and Vision Computing*, Vol.29, No.2-3, (2011), pp.79-103.
(17) A. K. Jain, *Fundamentals of Digital Image Processing*. Prentice-Hall, (1989).
(18) S. Ibaraki, W. Goto, A. Matsubara, T. Ochi, M. Hamamura, Self-calibration of a cross grid encoder, *Journal of the Japan Society for Precision Engineering*, Vol.72, No. 8, (2006), pp.1032-1037 (in Japanese).
(19) O. Sato, S. Osawa, and T. Takatsuji, Intercomparison of the calibration 2-D dimensional standard, *Proceedings of JSPE Spring Conference*, (2010), pp.375-376 (in Japanese).
(20) A. Matsubara, K. Nagaoka, and T. Fujita, Model-reference feedforward controller design for high-accuracy contouring control of machine tool axes, *CIRP Annals - Manufacturing Technology*, Vol.60, (2011), pp. 415-418.
(21) S. Yi, R. M. Haralick, and L. G. Shapiro. Error propagation in machine vision, *Machine*

Vision and Applications, Vol.7, (1994), pp.93–114.

(22) M. de Santo, C. Liguori, A. Paolillo, and A. Pietrosanto, Standard uncertainty evaluation in image-based measurements, *Measurement*, Vol.36, (2004), pp.347-358.

(23) R. Anchini, C. Liguori, and A. Paolillo, Evaluation of the uncertainty of edge detector algorithms, *IEEE Transactions on Instrumentation and Measurement*, Vol.56, No.3, (2007) pp.681-688.

(24) J. Ye, M. Takac, C. N. Berglund, G. Owen, and R. F. Pease, An exact algorithm for self-calibration of two-dimensional precision metrology stages, *Precision Engineering*, Vol.20, No.1, (1997) pp.16-32.